

ARTICLE

Received 17 Nov 2014 | Accepted 18 Sep 2015 | Published 23 Oct 2015

DOI: 10.1038/ncomms9669

OPEN

S-nitrosylation triggers ABI5 degradation to promote seed germination and seedling growth

Pablo Albertos¹, María C. Romero-Puertas², Kiyoshi Tatematsu³, Isabel Mateos¹, Inmaculada Sánchez-Vicente¹, Eiji Nambara⁴ & Oscar Lorenzo¹

Plant survival depends on seed germination and progression through post-germinative developmental checkpoints. These processes are controlled by the stress phytohormone abscisic acid (ABA). ABA regulates the basic leucine zipper transcriptional factor ABI5, a central hub of growth repression, while the reactive nitrogen molecule nitric oxide (NO) counteracts ABA during seed germination. However, the molecular mechanisms by which seeds sense more favourable conditions and start germinating have remained elusive. Here we show that ABI5 promotes growth via NO, and that ABI5 accumulation is altered in genetic backgrounds with impaired NO homeostasis. S-nitrosylation of ABI5 at cysteine-153 facilitates its degradation through CULLIN4-based and KEEP ON GOING E3 ligases, and promotes seed germination. Conversely, mutation of ABI5 at cysteine-153 deregulates protein stability and inhibition of seed germination by NO depletion. These findings suggest an inverse molecular link between NO and ABA hormone signalling through distinct posttranslational modifications of ABI5 during early seedling development.

¹Dpto. de Microbiología y Genética, Instituto Hispano-Luso de Investigaciones Agrarias (CIALE), Facultad de Biología, Universidad de Salamanca, C/ Río Duero 12, Salamanca 37185, Spain. ²Dpto. de Bioquímica, Biología Celular y Molecular de Plantas, Estación Experimental del Zaidín, Consejo Superior de Investigaciones Científicas, Profesor Albareda 1, Granada E-18008, Spain. ³Laboratory of Plant Organ Development, National Institute for Basic Biology, Nishigonaka 38, Myodaiji, Okazaki 444-8585, Japan. ⁴Department of Cell and Systems Biology, University of Toronto, 25 Willcocks Street, Toronto, Ontario, Canada M5S3B2. Correspondence and requests for materials should be addressed to O.L. (email: oslo@usal.es).

In the plant life cycle, the development of a new seedling depends on both appropriate timing of seed germination and the perception of environmental conditions. Consequently, germination and early seedling development must be tightly regulated by exogenous and endogenous signal molecules. Among them, abscisic acid (ABA) plays an important role in the inhibition of seed germination¹ and in post-germinative seedling arrest under unfavourable environmental conditions². ABA-dependent growth arrest after germination relies on the basic leucine zipper-type transcription factor ABI5 (refs 3–5). In many plant developmental processes and stress responses, the precise changes in cellular status are regulated not solely by ABA signalling but by a complex network of ABA and other signalling pathways. Several examples of cross-talk between ABA and the gaseous signalling molecule nitric oxide (NO) have been recently reported. These interactions include the link of SnRK2.6/OST1 S-nitrosylation to the negative regulation of ABA signalling in the stomata⁶ and the NO regulation of ABI5 transcription through control of group VII ethylene response factors (ERFs) stability⁷. NO is a signalling molecule involved in a variety of physiological processes during plant growth and development. Extensive research has shown that NO affects seed dormancy, seed germination and ABA sensitivity^{8,9}, as evidenced by exogenous application of NO donors¹⁰ or by genetic analysis of mutants with altered endogenous NO levels in *Arabidopsis*¹¹. However, despite the abundant involvement of NO in different plant cell signalling pathways, the actual knowledge about its direct targets is poorly understood. A key feature of NO biology is the posttranslational modification of cysteine thiol to form nitrosothiols (S-nitrosylation) in target proteins¹². In animals, this posttranslational modification has also been related to protein degradation via the ubiquitin-dependent proteasome pathway¹³. Here we establish a molecular mechanism for NO and ABA antagonism in the regulation of seed germination and post-germinative development through ABI5 protein stability. Genetic analysis identified that *abi5* mutants are insensitive to NO scavenging during seed germination. ABI5 protein levels are high in NO-deficient mutant backgrounds and low in NO-overaccumulating plants. S-nitrosylation of ABI5 at Cys 153 facilitates its degradation and promotes seed germination. Conversely, mutation of ABI5 Cys 153 reduces protein degradation through CULLIN4 (CUL4)-based and KEEP ON GOING E3 (KEG) ligases, and deregulates the inhibition of seed germination by NO depletion. Thus, ABI5 is regulated through the antagonistic action of ABA and NO, as evidenced by the synergistic effect of S-nitrosoglutathione (GSNO) on ABI5 destabilization. These findings suggest an inverse molecular link between NO and ABA hormone signalling through distinct posttranslational modifications of ABI5 during gene regulation of early seedling development.

Results

Identification and genetic characterization of *gap* mutants. NO affects seed dormancy, seed germination and ABA sensitivity^{8,9}, as shown by exogenous application of NO donors¹⁰ or by genetic analysis of mutants with altered endogenous NO levels in *Arabidopsis*¹¹. By exploiting the cross-talk between ABA and NO in the transition from dormancy to germination, we performed a genetic screen using (+)-S-ABA coupled to the effect of the NO scavenger 2-(4-carboxyphenyl)-4,4,5,5-tetramethylimidazole-1-oxyl-3-oxide (cPTIO). We isolated 7 (+)-S-ABA-insensitive mutants that were able to germinate on 3 μ M (+)-S-ABA and also display a cPTIO-insensitive phenotype (Supplementary Fig. 1a). These mutants were named *gap* (*germination in ABA and cPTIO*). Allelism tests indicated

that these fell into two different loci, five of these mutants corresponding to new *abi5* alleles verified by candidate gene sequencing (Supplementary Fig. 1b). Germination of Col-0 wild-type seeds was delayed by 100 μ M cPTIO (Fig. 1a,b), in agreement with previous reports⁹; however, germination of the *abi5* mutant alleles was less affected by NO depletion than the wild type. Hence, these results showed that *abi5* mutants were insensitive not only to ABA but also to NO scavenging by cPTIO during seed germination.

NO induces degradation of the ABI5 protein. To extend these findings, we determined the localization of the ABI5 protein (Fig. 1c) and ABI5 transcript (Fig. 1d) in seeds after treatment with ABA, the NO donor S-nitroso-N-acetyl-DL-penicillamine (SNAP) and the NO scavenger cPTIO. ABI5 accumulated to high levels after treatment with ABA for 48 or 72 h and even earlier after NO was depleted (Fig. 1d). In contrast, application of the NO donor SNAP quickly reduced ABI5-GUS levels (Fig. 1c and Supplementary Fig. 2).

To further investigate the role of NO in the regulation of seed germination in *Arabidopsis*, we examined endogenous NO levels in 2-day-old wild-type seeds by using the fluorescence indicator 4,5-diaminofluorescein diacetate (DAF-2DA). We observed NO-dependent fluorescence in the seed endosperm and rapid elongation zone after radicle protrusion (Fig. 1c), as previously described^{14,15}. Application of the NO scavenger cPTIO reduced the DAF-2DA fluorescence pattern in treated seeds, signal being limited to the autofluorescence of the testa tissues (Supplementary Fig. 1c–e). Co-localization of NO burst and ABI5 tissue-specific reduction of ABI5-GUS protein during radicle protrusion (seed imbibition/germination) was confirmed after GUS histochemical analysis using *pABI5:ABI5-GUS* lines as highlighted in Fig. 1c.

Recently, the N-end rule pathway of targeted proteolysis has been shown to regulate ABI5 expression through group VII ERF transcription factors⁷. To this end, application of MG132 did not transcriptionally induce ABI5 gene expression, as a putative consequence of enhanced group VII ERF stabilization (Fig. 2a).

The effect of SNAP and the physiological NO donor GSNO in the promotion of seed germination was correlated by the disappearance of ABI5 during germination and post-germinative growth (Fig. 2b–d and Supplementary Fig. 3a–c). Conversely, endogenous NO depletion by the cPTIO scavenger inhibited seed germination and maintained high ABI5 protein levels, similar to ABA (Fig. 2b,d). It is noteworthy that the proteasome inhibitor MG132 or the proteasome inhibitor cocktail (including MG115, MG132 and epoxomicin) restored ABI5 accumulation, even in the presence of NO donors, and prevented seed germination (Fig. 2b,c and Supplementary Fig. 3c). In addition, cycloheximide alongside the MG132 and NO donor/scavenger treatments proved that ABI5 protein stability was being affected (Fig. 2a,c). Collectively, these findings implied that NO function during seed germination was through ABI5 degradation. After this developmental checkpoint and at high concentrations, NO dramatically affected post-germinative seedling growth, inhibiting root growth and development¹⁵.

ABI5 level is altered when NO homeostasis is impaired. We corroborated the above pharmacological findings by the use of mutants and transgenic lines impaired in NO homeostasis. Thus, NO-deficient *atnoa1-2;nia1;nia2* triple mutant impaired in NIA/NR- and AtNOA1-dependent NO biosynthesis in *Arabidopsis* was hypersensitive to ABA, underscoring its effect on germination inhibition¹¹ (Supplementary Fig. 3d). Non-symbiotic

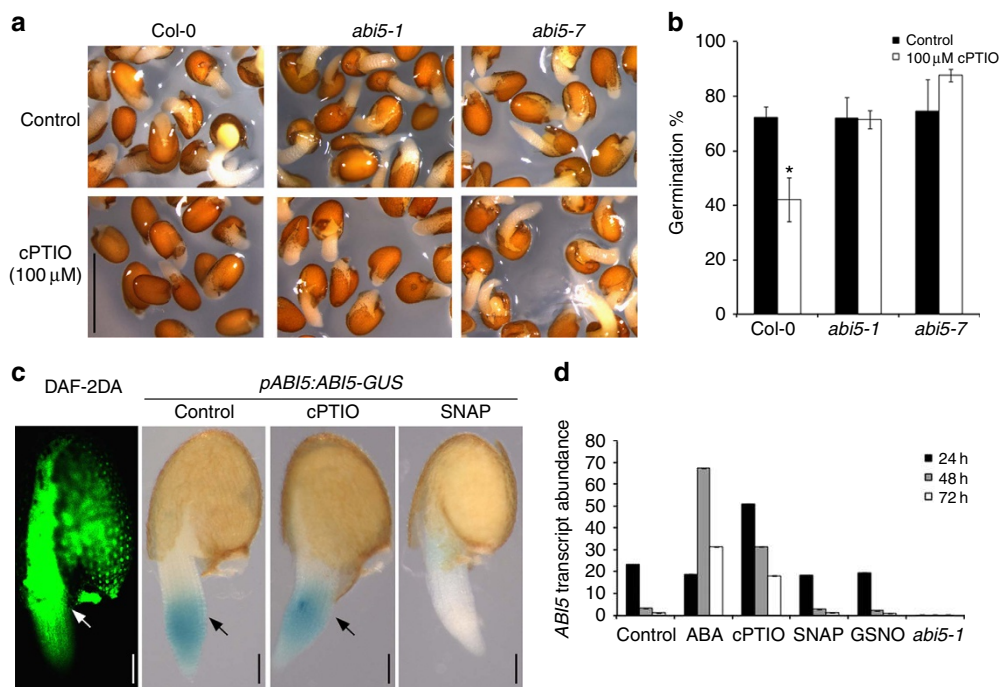


Figure 1 | NO depletion phenotypes of ABI5 loss-of-function mutants during seed germination. (a) Insensitivity of *abi5* mutants to NO scavenging by cPTIO during seed germination. Photographs of 2-day-old germinated seeds after imbibition of wild type (Col-0) and the ABA-insensitive *abi5-1* and *abi5-7* mutants, in the absence of (Control) or the presence of 100 μM cPTIO. Scale bar, 1 mm. (b) Germination of wild-type (Col-0), *abi5-1* and *abi5-7* seeds in media containing 0 and 100 μM cPTIO after 2 days. Error bars represent ± s.e. ($n=3$). Asterisk indicates significant differences compared with Col-0 (Control) (t -test, $P<0.05$). (c) Co-localization of ABI5 expression, protein localization and NO production. *pABI5:ABI5-GUS* seeds were stratified for 3 days at 4 °C and grown for 1 to 2 days at 21 °C on MS agar plates and then subjected to DAF-2DA incubation or GUS staining after treatment with NO scavenger (cPTIO) and donor (SNAP). Arrows indicate high NO accumulation (left), and ABI5 expression and protein localization (middle). Scale bars, 100 μm. (d) qRT-PCR analysis of ABI5 relative transcript abundance in Col-0 seeds untreated (Control) and after treatments with ABA, cPTIO, SNAP and GSNO after 24, 48 and 72 h and in the *abi5-1* background. Error bars represent ± s.e. ($n=3$).

haemoglobin 1 (AHb1) is an endogenous scavenger of NO, and thus AHb1-overexpressing and -silenced lines contain lower and higher NO levels, respectively¹⁶. As expected, the ABA response phenotype of these AHb1 lines during seed germination differed from the hypersensitivity to ABA of the AHb1-overexpressing lines to the wild-type germination of the AHb1-silenced lines (Supplementary Fig. 3e,f).

We investigated ABI5 protein accumulation in the *Arabidopsis atnoa1*, *nial1;nial2* and *atnoa1;nial1;nial2* mutant seeds, which exhibit decreased levels of cellular NO¹¹ (Fig. 2e). NO-deficient mutants, defective in either the oxidative or reductive NO synthesis pathways, respectively, or in both pathways, accumulated higher ABI5 protein levels. In agreement with the enhanced ABA sensitivity of NO-deficient mutant backgrounds, ABI5 protein levels were increased with respect to those observed in the wild type (Col-0). To corroborate these findings, AHb1-overexpressing and -silenced lines were also analysed for their ABI5 accumulation pattern (Fig. 2f). Collectively, these findings implied that genetic backgrounds where the endogenous NO levels were enhanced (AHb1-silencing lines) or diminished (*atnoa1*, *nial1;nial2*, *atnoa1;nial1;nial2* and AHb1-overexpressing lines) displayed altered ABI5 levels, which were mirrored by changes in their ABA response. These pharmacological and genetic approaches suggest that NO promoted ABI5 protein degradation via a proteasome-dependent pathway.

ABI5 is S-nitrosylated *in vivo* and *in vitro*. One possible mechanism of NO action in plant tissues is the redox-based posttranslational modification of target proteins through

S-nitrosylation. NO is able to reversibly modify thiol groups of specific cysteine residues in target proteins, hence altering protein function¹². To determine whether ABI5 was S-nitrosylated by NO, the recombinant protein was exposed to either GSNO or SNAP, which are typically used to evaluate S-nitrosylation (that is, SNO formation) *in vitro*¹⁷. The formation of SNO-ABI5 was monitored by the biotin switch method¹⁸. As shown in Fig. 3a–c, ABI5 was S-nitrosylated by either GSNO or SNAP. Furthermore, the addition of dithiothreitol (DTT) strongly reduced the formation of SNO-ABI5, consistent with the presence of a reversible thiol modification. The biotin switch was assayed without ascorbate, to assure that the immune reactivity of the protein was ascorbate dependent (Supplementary Fig. 4a) and to prevent switching SNO for biotin, as the method describes¹⁸. ABI5 contains four cysteine residues (Cys 56, Cys 153, Cys 293 and Cys 440) that might serve as sites for this redox-based modification (Supplementary Fig. 4b). *In-silico* prediction suggested that Cys 153 was potentially S-nitrosylated (Supplementary Fig. 4d,e). Mass spectrometry analysis confirmed S-nitrosothiol formation at only Cys 153 of ABI5 (Fig. 3a,b and Supplementary Figs 5 and 6). This residue was therefore mutated individually and the resulting protein was expressed and treated with GSNO before analysis with the biotin switch method. The Cys153 to Ser mutation abolished S-nitrosylation of ABI5 (Fig. 3c). Collectively, these findings indicated that Cys 153 of ABI5 was specifically S-nitrosylated *in vitro*. This Cys 153 is only present in the closest ABI5 homologue AtbZIP67 (Supplementary Fig. 4c), sharing a seed expression pattern with ABI5 (Supplementary Fig. 7). Together, these data suggest that redox modification by S-nitrosylation may regulate the activity of these

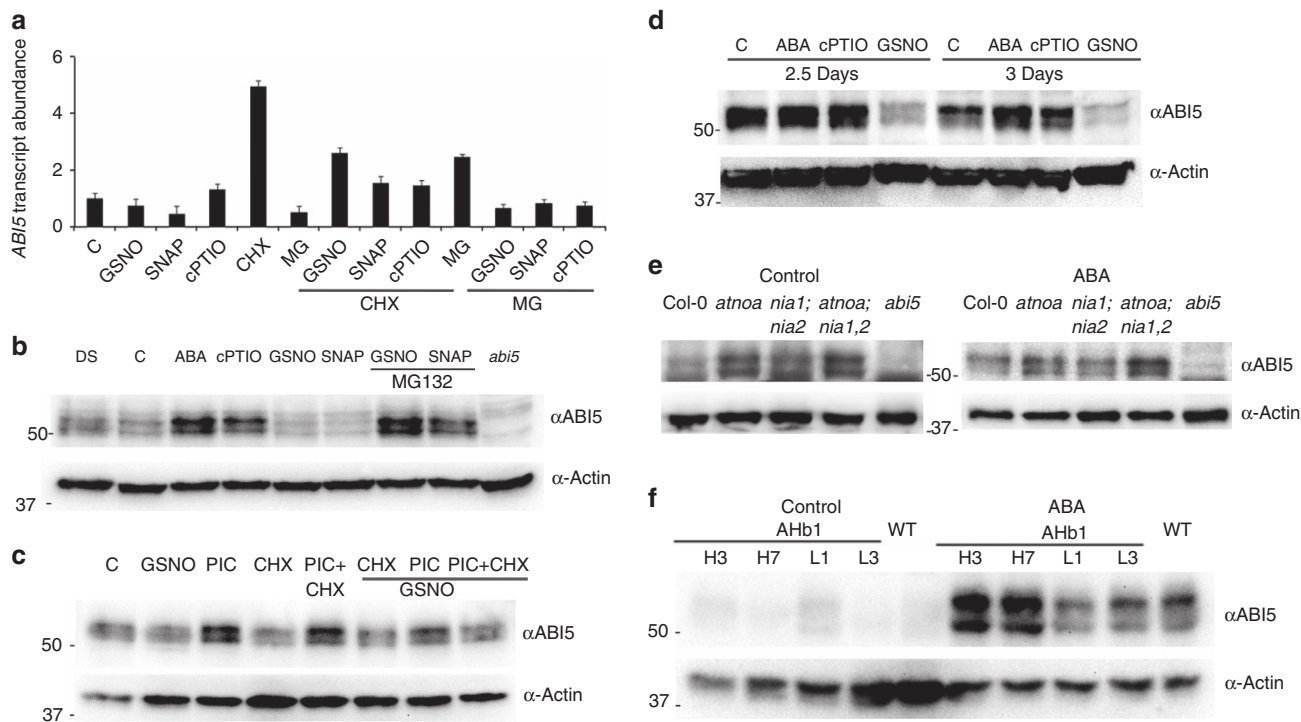


Figure 2 | Increased NO levels reduce ABI5 protein accumulation in a proteasome pathway-dependent manner. (a) qRT-PCR analysis of *ABI5* relative transcript abundance in Col-0 seeds untreated (C) and after treatments with GSNO, SNAP, cPTIO, cycloheximide (CHX), MG132 proteasome inhibitor and the combinations indicated after 3 h. Error bars represent \pm s.e. ($n = 3$). (b) SNAP and GSNO treatments promote ABI5 degradation in dormant seeds (DS). Immunoblot analysis of ABI5 protein levels in seed extracts of Col-0 and *abi5-1*, treated with or without (C) NO scavenger (cPTIO) and donors (GSNO and SNAP), and the MG132 proteasome inhibitor. Actin protein levels are shown as a loading control. (c) Immunoblot analysis of ABI5 protein levels in seed extracts of Col-0 dormant seeds treated with or without (C) NO donor (GSNO), the proteasome inhibitor cocktail (PIC, composed of MG115, MG132 and epoxomicin), cycloheximide (CHX) and the combinations indicated. Actin protein levels are shown as a loading control. (d) GSNO treatment promotes ABI5 degradation in 2 days ABA (5 μ M)-treated after-ripened seeds. Immunoblot analysis of ABI5 protein levels in seed extracts of Col-0, treated with or without (C) NO scavenger (cPTIO) and donor (GSNO). Actin protein levels are shown as a loading control. (e) ABI5 protein levels in wild type (WT; Col-0), *abi5-1* and NO-deficient (*atnoa1-1; nia1; nia2*, *atnoa1-2; nia1; nia2*) mutant backgrounds. Stratified seeds were sown on control MS (Control, left) and 0.1 μ M ABA after 48 h (right). Immunoblot analysis of ABI5 protein levels in seed extracts of WT and NO-deficient mutants. Actin protein levels are shown as a loading control. (f) ABI5 protein levels in WT, 35S:*AHb1* (H3, H7) and 35S:*antiAHb1* (L1, L3) lines. Stratified seeds were sown on MS (Control) and 0.1 μ M ABA for 96 h. Immunoblot analysis of ABI5 protein levels in seed extracts of *AHb1*-overexpressing and -silencing lines. Actin protein levels are shown as a loading control.

b-ZIP transcription factors in plants to govern seed germination and seedling establishment.

To understand whether S-nitrosylation of Cys 153 could modulate the function of ABI5, we assessed the effect of this NO-mediated posttranslational modification on the previously reported homodimerization of the ABI5 protein¹⁹ by using a yeast two-hybrid assay. Interestingly, neither the ability of ABI5 to interact (Supplementary Fig. 8) nor the DNA-binding capacity to the ABRE *cis*-consensus motif (Supplementary Fig. 9) were disturbed by the Cys-Ser mutation or in the presence of NO-related compounds.

To determine whether ABI5 was S-nitrosylated *in vitro* during seed germination, protein extracts from wild-type and 35S:*ABI5* transgenic plants were treated with GSNO and MG132, and assayed by the biotin switch method, then S-nitrosylated proteins were immunopurified (Fig. 3d,e). Protein gel blot analysis of purified proteins probed with an antibody specifically recognizing the ABI5 protein showed the corresponding S-nitrosylation *in vitro*. In addition, *in vivo* studies with transgenic ABI5 lines expressing either Myc-tagged wild-type ABI5 or mutant derivatives were analysed during seed germination and treatment with MG132. To this end, endogenous proteins were subjected to biotin-switch analysis, immunoprecipitated and detected with an

anti-ABI5 antibody. Wild-type ABI5 was S-nitrosylated during seed germination, but the Cys153Ser mutant was not (Fig. 3f). Therefore, these results suggest that NO may regulate ABI5 redox state by S-nitrosylation at Cys 153 during seed imbibition.

ABI5 is a NO sensor during seed germination. To assess a physiological role for S-nitrosylation of the ABI5 protein during seed germination, ABI5- and ABI5Cys153Ser-overexpressing lines were generated in *Arabidopsis* by expressing this protein under control of the 35S promoter, in the wild-type and *abi5-1* mutant background (Supplementary Fig. 10). The phenotype of the transgenic plants was evaluated in response to NO and ABA, and was compared with that of *abi5* mutant and 35S:*ABI5* transgenic plants. Intact ABI5- and mutated ABI5-Cys153Ser-overexpressing lines exhibited ABA-hypersensitive phenotypes during seed germination and seedling establishment (Supplementary Fig. 10d), demonstrating that ABI5Cys153Ser was able to largely restore the *abi5-1* mutation (Supplementary Fig. 10e). To further explore the possible biological consequence of ABI5-SNO formation at Cys 153, ABI5 protein accumulation was monitored in the presence of the protein synthesis inhibitor cycloheximide with or without GSNO (Fig. 4a). The data

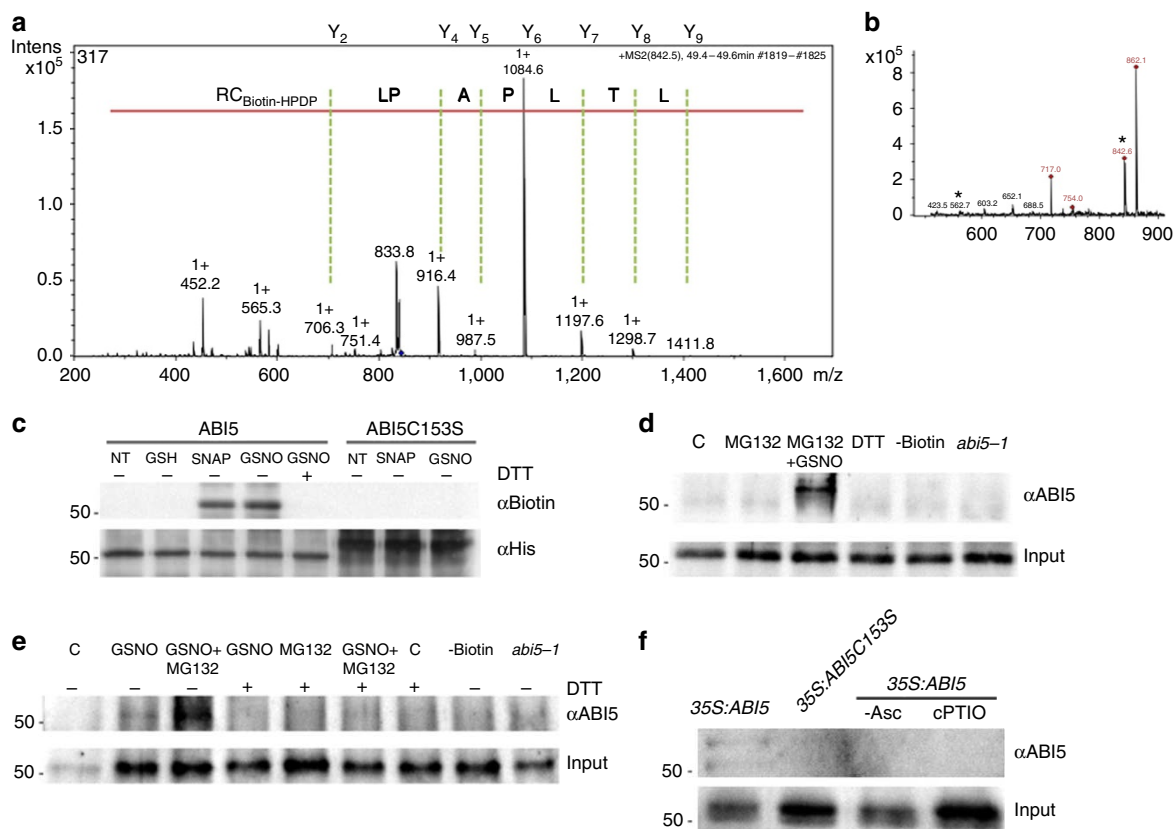


Figure 3 | S-nitrosylation of ABI5 in vivo and in vitro. (a) Mass spectrometric analyses identify C153 as the S-nitrosylation site. MS/MS spectra of C153 from the tryptic fragment QGSLTLPAPLPCR (peptide MS/MS spectra shown with Cys modified by biotin-HPDP). (b) The LC-MS spectra of the corresponding peaks (*562 m/z (3+) and 842.49 m/z (+2)) of this peptide fragment is shown in the inset. (c) The C153S mutation blocks S-nitrosylation of ABI5. *In vitro* S-nitrosylation of wild-type ABI5 and mutant ABI5C153S recombinant proteins by the NO donors GSNO (200 μM) and SNAP (200 μM). This modification is reversed by treatment with DTT (20 mM). No signal was observed with glutathione (200 μM) treatment showing specificity of the biotin-switch assay. ABI5 protein loading was detected by anti-His antibody. (d,e) S-nitrosylation of ABI5 induced by GSNO in after-ripened seed extracts. Samples were initially immunopurified with anti-biotin before immunoblot analysis of ABI5 protein levels in seed extracts of Col-0 (d), *35S:ABI5* (e) and *abi5-1* untreated (C) or treated with the indicated compounds. No signal was observed in the absence of biotin (– Biotin) or after DTT (20 mM) treatment. Actin protein levels are shown as a loading control. (f) *In-vivo* S-nitrosylation of ABI5 in *abi5-1*; *35S:cMyc-ABI5* and *abi5-1*; *35S:cMyc-ABI5C153S* after-ripened seed extracts 24 h after proteasome inhibitor MG132 (100 μM) incubation. Immunoblot analysis of *in vivo* ABI5 protein levels after immunopurification of S-nitrosylated proteins. No signal was observed in the absence of sodium ascorbate (– Asc) or after cPTIO (1 mM) treatment. Input protein levels were also determined using anti-ABI5 anti-serum.

obtained implied that the mutation of ABI5 at Cys 153, considering similar seed germination stages, impaired NO-promoted ABI5 degradation, resulting in elevated levels of ABI5 protein. CUL4 and KEG are well-known factors that directly bind and regulate ABI5 ubiquitin-mediated proteolysis^{20–24}. Accordingly, mutations in either CUL4 or KEG abolished NO-promoted ABI5 protein degradation (Fig. 4b and Supplementary Fig. 11). Intact ABI5 protein interacted with both CUL4 and KEG in the presence of GSNO, whereas ABI5Cys153Ser mutation failed to interact (Fig. 4c,d), supporting that S-nitrosylation triggered ABI5 destabilization through CUL4-based and KEG E3 ligases.

To determine the possible impact of the ABI5Cys153Ser mutation on NO sensing during seed germination and seedling establishment, we treated intact *ABI5*- and mutated *ABI5Cys153Ser*-overexpressing lines with NO scavengers (cPTIO) and donors (SNAP) (Fig. 4e,f and Supplementary Fig. 10f). As depicted in Fig. 4e,f, inhibition of seed germination by NO depletion during radicle protrusion was enhanced in *ABI5* but not in *ABI5Cys153Ser* overexpressors and also in the establishment of a new plant (Supplementary Fig. 10f), resulting in a prominent decrease in the rate of germination. In addition, there was a significant increase

in seedling establishment after NO treatment in the *ABI5*-overexpressing lines relative to the overexpression of the *ABI5Cys153Ser* mutant version that instead was able to maintain growth arrest (Supplementary Fig. 10f). Germination of the transgenic plants under unfavourable conditions such as high salinity and hyperosmotic stress showed NaCl- and mannitol-hypersensitive inhibition of post-germinative growth in *35S:ABI5* and *35S:ABI5C153S* lines as compared with wild-type plants (Fig. 4g). Indeed, *35S:ABI5C153S* lines were more deeply hypersensitive than the *ABI5*-overexpressing lines. Together, this information implies that one way in which seeds sense NO was by the S-nitrosylation of ABI5 at Cys 153, and that disruption of this mechanism was able to arrest seedling growth under adverse environmental conditions.

The involvement of group VII ERF transcription factors in NO sensing and NO downregulation of *ABI5* transcription has been previously reported⁷. Consistently, ABI5 protein levels accumulated to a greater extent after ABA treatment in *prt6-1* mutant seeds and seedlings, which are impaired in the degradation of group VII ERFs by the N-end rule pathway^{25,26} (Fig. 5a–c). Thus, Rubisco large subunit was detected in those

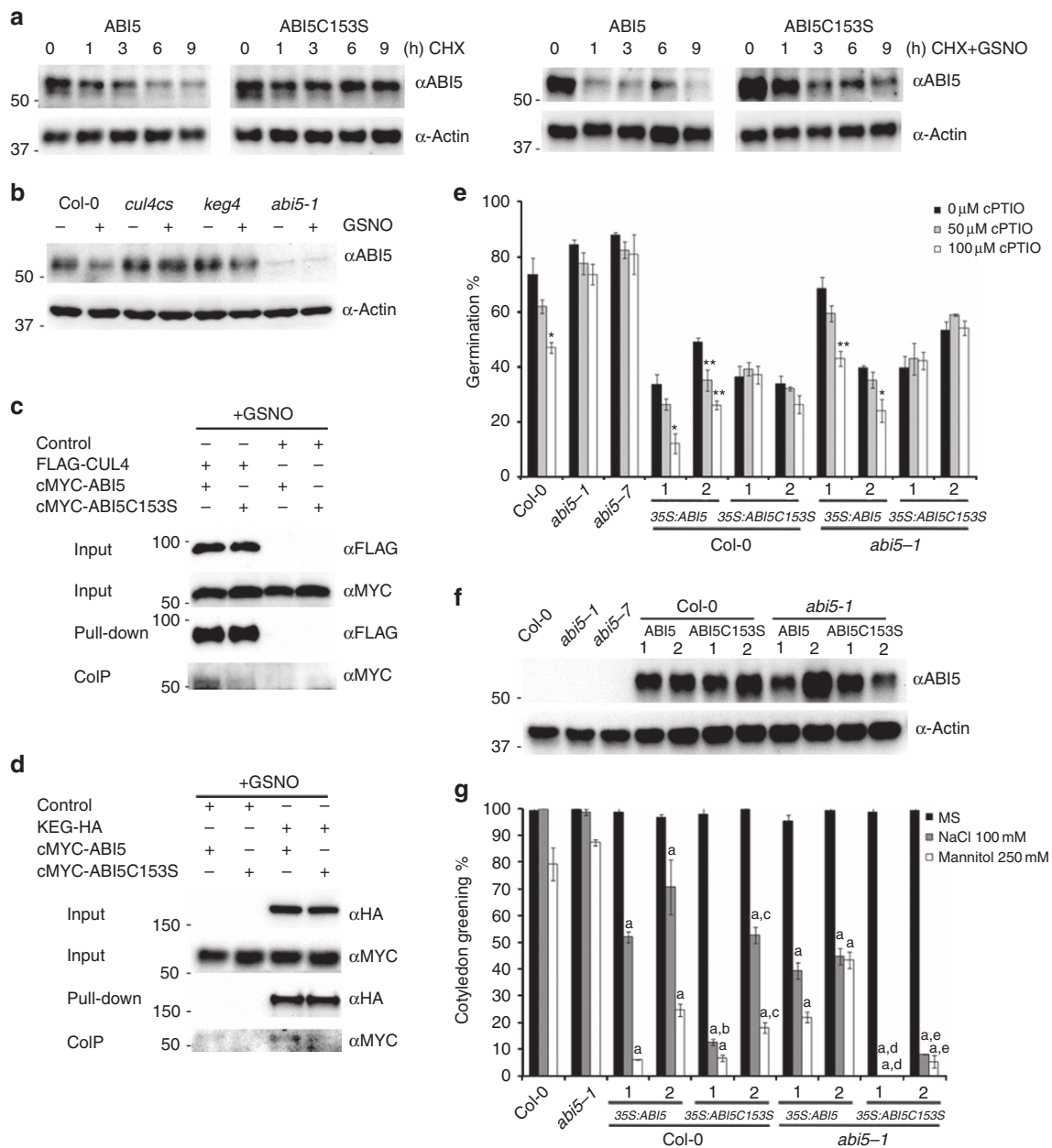


Figure 4 | The ABI5 C153S mutant shows decreased proteasomal degradation by CUL4 and KEG, and confers NO insensitivity during seed germination. (a) Immunoblot analysis of ABI5 protein levels in 8-day-old seedling extracts of similar germination stages *abi5-1*;35S:cMyc-ABI5 and *abi5-1*;35S:cMyc-ABI5C153S, in the presence of cycloheximide (1 mM) and cycloheximide (1 mM) plus GSNO (500 μ M) from 0 to 9 h. Actin protein levels are shown as a loading control. (b) ABI5 protein levels in wild type (Col-0), *cul4cs*, *keg4* and *abi5-1* mutant backgrounds. Stratified seeds were incubated with 5 μ M ABA for 48 h and treated with GSNO (1 mM) for 6 h after ABA removal. Immunoblot analysis of ABI5 protein levels in seed extracts of wild type and mutants. Actin protein levels are shown as a loading control. (c) Co-immunoprecipitation assays between CUL4 and transgenic ABI5/ABI5C153S proteins in the presence of GSNO. Input protein levels were also determined using anti-FLAG and anti-MYC antisera, respectively. (d) Co-immunoprecipitation assays between KEG and ABI5/ABI5C153S proteins in the presence of GSNO. Input protein levels were also determined using anti-HA and anti-MYC antisera, respectively. (e) NO-insensitive inhibition of seed germination to NO scavenging in 35S:ABI5C153S lines as compared with 35S:ABI5 plants. Total seed germination of wild type (Col-0), *abi5-1*, *abi5-7* and two (1, 2) 35S:ABI5- and 35S:ABI5C153S-independent lines grown for 2 days on MS agar plates untreated (Control) or supplemented with 50 and 100 μ M of the NO-scavenger cPTIO. Values represent the mean \pm s.e. ($n = 3$). Asterisks indicate significant differences compared with 0 μ M cPTIO (t -test, * $P < 0.05$, ** $P < 0.01$). (f) ABI5 levels in 35S:ABI5 and 35S:ABI5C153S transgenic lines used for the germination assay. Immunoblot analysis of ABI5 protein levels in seed extracts. Actin protein levels are shown as a loading control. (g) NaCl- and mannitol-hypersensitive inhibition of post-germinative growth in two 35S:ABI5 and 35S:ABI5C153S lines as compared with wild-type plants. Seedling growth of wild type (Col-0), *abi5-1*, 35S:ABI5 and 35S:ABI5C153S lines grown for 9 days on MS agar plates untreated (Control) or supplemented with 100 mM of NaCl and 250 mM of mannitol. Values represent the mean \pm s.e. ($n = 3$). Letters indicate significant differences compared with wild-type (Col-0) (a), 35S:ABI5-1 (b), 35S:ABI5-2 (c), *abi5-1*;35S:ABI5-1 (e), *abi5-1*;35S:ABI5-2 (d), (t -test, $P < 0.05$).

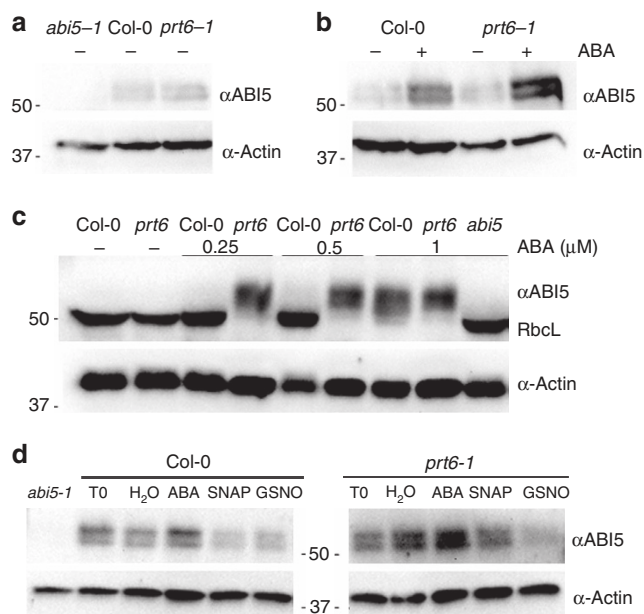


Figure 5 | ABI5 accumulation and degradation in *prt6-1* mutant background during seed germination and post germination. (a,b) ABA treatment promotes ABI5 accumulation in germinating seeds. Immunoblot analysis of ABI5 protein levels in seed extracts of Col-0 and *prt6-1* before (a) and after 48 h treatment with (+) or without (–) 0.25 μM ABA (b). Actin protein levels are shown as a loading control. (c) Post-germinative ABI5 accumulation in seedlings. Immunoblot analysis of ABI5 protein levels in 10-day-old extracts of Col-0, *prt6-1* and *abi5-1*, treated with or without (–) 0.25, 0.5 and 1 μM ABA. Actin protein levels are shown as a loading control and Rubisco large subunit (RbcL) detection is indicated. (d) ABI5 protein levels in wild-type (Col-0), *prt6-1* and *abi5-1* mutant backgrounds. Stratified seeds were incubated with 5 μM ABA for 48 h (T0) and treated after ABA removal with H₂O, ABA, SNAP (1 mM) and GSNO (1 mM) for 12 h. Immunoblot analysis of ABI5 protein levels in seed extracts of wild type and mutants. Actin protein levels are shown as a loading control.

conditions/genotypes where the development of green and expanded cotyledons had taken place, producing seedlings with the ability to fix carbon during photosynthesis (Fig. 5c). The key role of ABA in the inhibition of seed germination and in post-germinative seedling arrest (that is, the absence of green and expanded cotyledons) was also highlighted, as no detection of Rubisco large subunit could be found in those ABA-hypersensitive genotypes (*prt6*) or in the Col-0 wild type under high ABA concentrations. Conversely, ABI5 was only detected in those conditions/genotypes where the seed germination was inhibited and/or seedling growth arrested at post-germination developmental checkpoints. Here we also demonstrated that NO-induced ABI5 degradation by the proteasome could occur in a *prt6-1* mutant background (Fig. 5d). Thus, NO could promote ABI5 protein degradation independently of the NO-dependent transcriptional control of *ABI5* by the N-end rule pathway. Taken together, our results demonstrated a pivotal role of ABI5 in antagonistic ABA and NO signalling in the regulation of seed germination and highlighted ABI5 as a critical NO sensor in seeds.

Discussion

In conclusion, our data establish a molecular mechanism for NO and ABA antagonism in the regulation of seed germination and post-germinative growth (Fig. 6). We identify two new loci

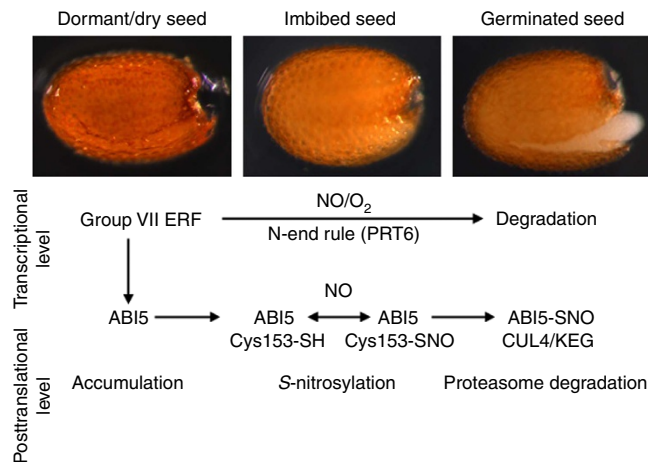


Figure 6 | Model showing a role for NO in the regulation of ABI5 during seed germination. Transcriptional control of *ABI5* expression via the group VII ERFs⁷ and posttranslational S-nitrosylation of ABI5 protein are included. Dormant and dry seeds accumulate high levels of the ABA-induced ABI5 growth repressor. On seed imbibition, a burst of NO is early produced to degrade group VII ERFs via the N-end rule pathway of targeted proteolysis (PRT6)^{25,26} and induces ABI5 S-nitrosylation promoting the interaction with CUL4-based and KEG E3 ligases. Consequently, ABI5 is rapidly degraded by the proteasome during seed germination.

involved in ABA and NO signalling (*GERMINATION IN ABA AND cPTIO, GAP*) and characterize one of these loci that correspond to the basic leucine zipper transcription activator ABI5. S-nitrosylation of ABI5 targets proteasomal degradation through CUL4-based and KEG ligases and acts as a regulatory switch for seed germination in *Arabidopsis*. Thus, S-nitrosylation offers new insights into the regulation of protein stability through CULLIN-related degradation pathways in plants.

The findings by Gibbs *et al.*⁷ and those reported here demonstrate that NO targets ABI5 at both the transcriptional level (through NO-mediated degradation of ERFVIIIs) and the posttranslational level (through NO-mediated degradation of ABI5), respectively, highlighting the fact that ABI5 is depleted via a dual NO-responsive mechanism. These two independent mechanisms converging on ABI5 may have evolved to ensure that NO irrevocably removes ABI5 from the seed to promote germination. Several previous reports emphasize that ABI5 protein stability is regulated tightly by multiple different mechanisms^{21–24}. Thus, it is reasonable to speculate that S-nitrosylation-mediated ABI5 protein degradation plays an important role in the NO function to regulate seed germination, rather than only through transcriptional regulation⁷. In addition, it is likely to be that other mechanisms of NO-induced ABI5 degradation independently of C153 S-nitrosylation may be involved, probably nitrosylating different regulators for ABI5 degradation.

The identification of ABI5 as a direct NO target involved in NO-mediated effects in plant growth and development contributes to our understanding of NO role in plant signal transduction networks and establishes a molecular framework for the NO function during seed germination.

Methods

Plant materials and treatments. *Arabidopsis thaliana* ecotype Columbia-0 (Col-0) was the genetic background for all wild-type plants used in this work. Seed stocks of *abi5*, *atnoa1*, *nia1;nia2* and *keg4* mutants were obtained from *Arabidopsis* Biological Resource Center. The *atnoa1;nia1;nia2* mutants¹¹ and 35S:*AHb1* (H3, H7) and 35S:*antiAHb1* (L1, L3) lines²⁷ were kind gifts from Dr José León

(IBMCP-CSIC, Valencia, Spain) and Dr Massimo Delledonne (University of Verona, Verona, Italy), respectively. Dr Xing Wang Deng (Yale University, Connecticut, USA) kindly provided *cul4cs* and *35S:FLAG-CULA* lines²⁰. DEX::KEG-HA lines were previously described²⁸.

Arabidopsis plants were grown in a growth chamber or greenhouse under 50–60% humidity, a temperature of 22 °C and with a 16-h light/8-h dark photoperiod at 80–100 $\mu\text{E m}^{-2} \text{s}^{-1}$ in pots containing a 1:3 vermiculite/soil mixture.

For *in vitro* culture, *Arabidopsis* seeds were surface sterilized in 75% (v/v) sodium hypochlorite and 0.01% (v/v) Triton X-100 for 5 min, and washed three times in sterile water before sowing. Seeds were stratified for 3 days at 4 °C and then sowed on Murashige and Skoog (MS)²⁹ solid medium with 2% (w/v) Suc and 0.6% (w/v) agar, and the pH was adjusted to 5.7 with KOH before autoclaving. Seeds were sown in different treatments and plates were sealed and incubated in a controlled environment growth chamber. For NO treatments, *Arabidopsis* seeds were sown in MS medium supplemented with 300 μM NO donors GSNO and SNAP or 300 μM 2-(4-carboxyphenyl)-4,4,5,5-tetramethylimidazole-1-oxyl-3-oxide (cPTIO) NO scavenger. MG132 proteasome inhibitor (100 μM) and 0.1–5 μM of ABA were used. Whenever required, seeds were transferred every 24 h to a new medium containing fresh compounds. At the end of the treatment, tissues were collected and frozen (–80 °C).

NO donors (SNAP and GSNO), NO scavenger (cPTIO), proteasome inhibitor (MG132), cycloheximide and ABA were purchased from Sigma.

Mutant screening. M2 seeds of ethyl methane sulfonate-mutagenized Columbia, ethyl methane sulfonate-mutagenized Landsberg *erecta* and fast neutron-mutagenized Columbia were purchased from Lehle Seeds (Round Rock, TX) and each of ~20,000 M2 seeds (20 batches of ~1,000 M2 seeds harvested from ~1,000 M1 seeds) was used for screening to isolate ABA- and cPTIO-insensitive mutants. Screening conditions were described previously³⁰, except for (+)-S-ABA and cPTIO were used. Briefly, M2 seeds were surface sterilized, sown on 0.8% agar plates supplemented with half strength of MS and 3 μM (+)-S-ABA or 100 μM cPTIO. Seeds were stratified for 4 days and incubated in the presence of ABA for 4 days at room temperature under continuous light condition. Germination in cPTIO was tested under continuous light conditions at room temperature without stratification. Seedlings were transferred to hormone-free media, incubated for several days and transferred to pots for seed harvest.

Germination assays. To measure ABA, cPTIO, NaCl and mannitol sensitivity, seeds were plated on solid medium composed of MS basal salts, 2% (w/v) Suc or 0.8% w/v agar plates (adjusted to pH 5.8 by 2-(N-Morpholino)ethanesulfonic acid buffer) and different concentrations of ABA (0.1–1 μM), cPTIO (100 μM), SNAP (300 μM), NaCl (100 mM) and mannitol (250 mM). Seed lots to be compared were harvested on the same day from individual plants grown under identical environmental conditions. Each value represents the average germination percentage of 50–100 seeds with the s.e. of three replicates. Experiments were repeated at least three times. For the dormancy assay, seed lots to be compared were freshly harvested on the same day from individual plants grown under identical environmental conditions and sown immediately without stratification. The after-ripening status of dry seed lots was determined following storage for 1–4 weeks. The percentage of seeds with an emerged radicle (germination) or seedlings that germinated and developed green, fully expanded cotyledons was determined every day during 10 days after sowing.

Detection of endogenous NO. One- to 3-day-old seeds were incubated in a 500- μl solution containing 5 μM of DAF-2DA (Sigma) in buffer Tris–HCl 10 mM, pH 7.4, during 1 h at 25 °C in the dark. Seedlings were then washed three times for 15 min with fresh buffer Tris–HCl 10 mM, pH 7.4. Finally, fluorescence emitted by DAF-2DA was detected on a Leica magnifying glass by excitation at 495 nm and emission at 515 nm. NO depletion was also achieved by adding the scavenger cPTIO (1 mM) to the solution.

GUS histochemical staining. GUS staining of *ABI5_{pro}:ABI5-GUS* seeds and seedlings was performed as previously described³¹ using 50 mM potassium phosphate buffer (pH 7.0) containing 0.05% (v/v) Triton X-100, 1 mM $\text{K}_3\text{Fe}(\text{CN})_6$, 1 mM $\text{K}_4\text{Fe}(\text{CN})_6$, 0.05 M EDTA and 1 mg ml^{-1} X-Gluc (Duchefa). Twenty-four-hour *Arabidopsis* germinated seeds in MS medium as well as endosperms from imbibed seeds with embryo removed after GSNO (1 mM), cPTIO (1 mM) and control (MetOH) treatment were used. Staining was examined after 2 h incubation at 37 °C for germinated seeds and 48 h for endosperms. Samples were mounted in 50% glycerol for imaging.

Quantitative reverse transcriptase-PCR analysis. Total RNA for quantitative reverse transcriptase-PCR (qRT-PCR) was extracted from 1- to 3-day-old *Arabidopsis* seeds treated with GSNO (300 μM), SNAP (300 μM), cPTIO (300 μM), ABA (5 μM), cycloheximide (1 mM), MG132 (100 μM) and control condition as previously described³². Briefly, frozen tissue was powdered with mortar and pestle, and incubated on ice with 550 μl of extraction buffer (0.4 M LiCl, 0.2 M Tris, pH 8, 25 mM EDTA, 1% SDS) and 550 μl chloroform followed by centrifugation for 3 min at 15,800g at 4 °C. Next, 500 μl of water-saturated acidic phenol and 200 μl of

chloroform were added to the supernatant. After centrifugation for 3 min, 1/3 volume of 8 M LiCl was used for precipitation at –20 °C for 1 h before centrifugation again for 30 min at 4 °C. Pellet was dissolved in 26 μl Diethyl pyrocarbonate treated water and incubated with 10 units of RNase-free DNase I (Roche) 30 min at 37 °C. RNA was precipitated in 3 M NaAc, pH 5.2, and ethanol, washed with 70% ethanol and resuspended in 20 μl Diethyl pyrocarbonate treated water. For 7-day-old *abi5-1;35S:cMyc:ABI5*, *abi5-1;35S:cMyc:ABI5C153S*, *Col-0;35S:cMyc:ABI5* and *Col-0;35S:cMyc:ABI5C153S* *Arabidopsis* seedlings, total RNA was extracted using TRIzol Reagent as directed by the manufacturer (Invitrogen) and complementary DNA was synthesized using SuperScript Kit (Roche). qRT-PCRs were performed as described previously¹⁵ in ABI PRISM 7000 Sequence Detection System (Applied Biosystems, Framingham, MA, USA). Amplification was carried out with 'Brilliant SYBR Green QPCR MasterMix' (Stratagene) according to the manufacturer's instructions. The thermal profile for SYBR Green real-time PCR was 50 °C for 2 min, 95 °C for 10 min, followed by 40 cycles of 95 °C for 15 s and 60 °C for 1 min. To generate the standard curves, cDNA isolated from *Arabidopsis* seedlings was serially diluted 10 \times and aliquots of the dilutions were used in standard real-time PCRs. Each value determination was repeated three times, to ensure the slope of the standard curves and to determine the s.d. The concentration of unknown samples was calculated with the ABI-Prism 7000 SDS software, which created threshold cycle values (C_t) and extrapolated relative levels of PCR product from the standard curve. Primers used were *ABI5* (forward 5'-AACATGCATTGGCGGCGAGT-3', reverse 5'-TTGTGCCCTTGACTTCAAAC-3') and *ACTIN8* (forward 5'-AGTGGTCGTACAACCGGTATGTT-3', reverse 5'-GAGGATAGCATGTGGAGTGAGAA-3') as a control.

Production of recombinant proteins and polyclonal antibodies. Wild-type *ABI5* (kindly provided by Dr Luis Lopez-Molina, University of Geneva, Geneva, Switzerland) and mutated *ABI5C153S* cDNAs were recombined into pET-28a⁺ vector, to obtain fusion proteins with amino-terminal His-tag. Recombinant proteins were expressed in *Escherichia coli* and purified using His-Select Nickel Affinity Gel (IMAC) (Sigma) according to the manufacturer's protocols (Biomedal).

A primary dose of 750 μg purified recombinant protein 6 \times His-ABI5 was emulsified in Freund's complete adjuvant (Sigma) and administered subcutaneously in two rabbits. Three doses of the protein (375 μg) emulsified in Freund's incomplete adjuvant (Sigma) were administered at intervals (21 days). After the third booster injection (10 days), blood was collected from the rabbits and the serums were separated. Antibodies (anti-ABI5) were isolated by column chromatography with a protein-G column (GE Healthcare Life Sciences).

Western blotting. Total protein for western blot analysis was extracted from dormant seeds of *Col-0*, *abi5-1* and after-ripened seeds of *Col-0*, *abi5-1* and transgenic lines untreated or treated during 72 h with ABA, cPTIO, GSNO, SNAP, GSNO and SNAP plus MG132 or the proteasome inhibitor cocktail including MG115 (1 μM), MG132 (100 μM) and epoxomicin (0.75 μM). For cycloheximide treatments, transgenic plants were germinated and grown on MS liquid medium during 7 days and cycloheximide (1 mM) alone or in combination with GSNO (500 μM) was added to the medium, and samples were taken at indicated intervals. Tissue was powdered using mortar and pestle, and incubated for 10 min on ice with extraction buffer (50 mM Tris–HCl, pH 7.5, 75 mM NaCl, 15 mM EGTA, 15 mM MgCl_2 , 1 mM DTT, 0.1% Tween 20, 1 mM NaF, 0.2 M NaV, 2 mM Na-pyrophosphate, 60 mM β -glycerolphosphate and 1 \times proteases inhibitor mix, Roche) followed by centrifugation for 10 min at 15,800g at 4 °C. Protein concentration was determined by the Bio-Rad Protein Assay (Bio-Rad) based on the Bradford method³³. Sixty micrograms of total protein was loaded per well in SDS-acrylamide/bisacrylamide gel electrophoresis using Tris–glycine–SDS buffer. Proteins were electrophoretically transferred to an Immobilon-P polyvinylidene difluoride membrane (Millipore) using the Trans-Blot Turbo (Bio-Rad). Membranes were blocked in Tris buffered saline-0.1% Tween 20 containing 5% Blocking Agent and probed with antibodies diluted in blocking buffer. Anti-ABI5 Purified Rabbit Immunoglobulin (Biomedal, 1:5,000), anti-Actin clone 10-B3 Purified Mouse Immunoglobulin (Sigma A0480, 1:20,000), monoclonal anti-polyHistidine – Peroxidase produced in mouse (Sigma A7058, 1:2,000) and ECL-Peroxidase-labelled anti-rabbit (Amersham NA934, 1:20,000) and anti-mouse (Amersham NA931, 1:20,000) antibodies were used in the western blot analyses. Detection was performed using ECL Advance Western Blotting Detection Kit (Amersham) and the chemiluminescence was detected using an Intelligent Dark-Box II, LAS-1000 scanning system (Fujifilm). Quantification of band intensity was performed with ImageJ software. Full-sized uncropped immunoblots of cropped blottings used in figures are included in Supplementary Fig. 12.

Site-directed mutagenesis. Site-directed mutagenesis of *ABI5* was performed using the QuickChange II Site-Directed Mutagenesis Kits (Stratagene Corporate). Plasmid pET28a-*ABI5* was used as template and primers were designed using the tools from Stratagene and synthesized by Isogen. The primers were as follows: forward primer: 5'-CACTTCCAGCTCCGCTTAGTAGGAAGACTGTTGAT-3' and reverse primer 5'-ATCAACAGTCTTCTACTAAGCGGAGCTGGAAGTG-3'. Mutations were confirmed by sequencing.

In vivo and in vitro S-nitrosylation assays. We used the biotin switch method¹⁸ that converts –SNO into biotinylated groups, to detect S-nitrosylated proteins in *Arabidopsis* seed extracts and recombinant purified ABI5 and ABI5C153S, with slight modification.

For *in vitro* S-nitrosylation, purified ABI5 recombinant protein was pre-treated with NO donors SNAP and GSNO (200 μ M, Calbiochem), and the glutathionylating agent glutathione (200 μ M, Sigma) in the dark at room temperature for 30 min with regular vortexing. Treatment with the reducing agent (DTT, 20 mM; Sigma) after GSNO incubation was carried out for 1 h under the same conditions, to check reversibility of the modification. Reagents were removed by precipitation with two volumes of cold acetone and proteins were assayed by the biotin switch method.

In vivo S-nitrosylation of ABI5 was carried out with *Arabidopsis* dry seeds homogenized in extraction buffer (50 mM Tris–HCl, pH 7.5, 75 mM NaCl, 15 mM EGTA, 15 mM MgCl₂, 0.1% Tween 20, 1 mM NaF, 0.2 M NaV, 2 mM Na-pyrophosphate, 60 mM β -glycerolphosphate) containing Complete Protease Inhibitor Cocktail (Roche). Seeds extracts (1 mg) were incubated with GSNO (1 mM) and proteasome inhibitor MG132 (100 μ M) in the dark for 30 min with repeated vortexing. Samples treated with DTT (20 mM) were also kept for 1 h under the same conditions and were used as a negative control. Proteins were recovered by precipitation with two volumes of acetone for 20 min at -20°C , to remove excess of GSNO/DTT and assayed by the biotin switch method.

For the biotin switch, extracts or recombinant proteins were incubated with 20 mM S-methyl-methanethiosulfonate and 2.5% SDS at 50°C for 30 min with frequent vortexing, to block free Cys. S-methyl-methanethiosulfonate was removed by protein precipitation with two volumes of cold acetone and proteins were dissolved in 0.1 ml of RB buffer (25 mM Hepes, 1 mM EDTA and 1% SDS, pH 7.7) per mg of protein. After addition of 1 mM HPDP biotin (Pierce, Rockford, IL) and 1 mM ascorbic acid, the mixture was incubated for 1 h at room temperature in the dark with intermittent vortexing. *In vivo* biotinylated proteins were purified by immunoprecipitation with neutravidin or an IPA (protein A/G Ultralink Resin, Pierce) anti-biotin antibody, overnight at 4°C with 15 μ l IPA per mg of protein, preincubated with 2 μ l of anti-biotin antibody (Sigma B7653, 1:2,000) as described elsewhere³⁴. Briefly, beads were washed three times with HEN buffer (100 mM Hepes, 1 mM EDTA and 0.1 mM neocuproine, pH 7.8) and bound proteins were eluted with 10 mM DTT in SDS–PAGE solubilization buffer, loaded in 10% SDS–PAGE and transferred to a polyvinylidene difluoride membrane, to detect ABI5 with anti-ABI5 Purified Rabbit Immunoglobulin (Biomedal, 1:5,000). *In vitro* biotinylated proteins with SDS–PAGE solubilization buffer were loaded in 12% SDS–PAGE, visualized by Brilliant Blue-G Colloidal Stain (Sigma) and protein bands were analysed by matrix-assisted laser desorption/ionization–tandem time of flight (MALDI–TOF/TOF). Alternatively, purified proteins were analysed directly by nano-liquid chromatography (LC) and ion-trap tandem mass spectrometry (MS/MS).

Mass spectrometry. For tryptic digestion in reducing conditions, Coomassie-stained bands were excised manually, deposited in 96-well plates and processed automatically in a Proteiner DP (Bruker Daltonics, Bremen, Germany). The digestion protocol³⁵ was used with minor modifications. Gel plugs were washed first with 50 mM ammonium bicarbonate and second with acetonitrile (ACN) before reduction with 10 mM DTT in 25 mM ammonium bicarbonate solution, and alkylation was carried out with 55 mM iodoacetamide in 50 mM ammonium bicarbonate solution. Gel pieces were then rinsed with 50 mM ammonium bicarbonate and with ACN, and then dried under a stream of nitrogen. Modified porcine trypsin (sequencing grade; Promega, Madison, WI) was added at a final concentration of 16 ng μ l⁻¹ in 25% ACN/50 mM ammonium bicarbonate solution and the digestion was led to proceed at 37°C for 6 h. The reaction was stopped by adding 0.5% trifluoroacetic acid for peptide extraction. Digestion in non-reducing conditions was done essentially with the same protocol, but no DTT and iodoacetamide were used. In both cases, tryptic peptides were dried by speed-vacuum centrifugation and resuspended in 4 μ l of MALDI solution (30% ACN + 15% isopropanol + 0.1% trifluoroacetic acid). Twenty per cent of each peptide mixture was deposited onto a 386-well OptiTOF Plate (Applied Biosystems) and allowed to dry at room temperature. A 0.8- μ l aliquot of matrix solution (3 mg ml⁻¹ CHCA in MALDI solution) was then added onto the dried digests and allowed to dry at room temperature.

For MALDI peptide mass fingerprinting (PMF) and MS/MS analysis, samples were automatically processed in an Abi 4800 MALDI–TOF/TOF mass spectrometer (Applied Biosystems) in positive ion reflector mode (ion acceleration voltage was 25 kV for MS acquisition and 1 kV for MS/MS) and the spectra were stored into the Abi 4000 Series Explorer Spot Set Manager. PMF and MS/MS fragment ion spectra were smoothed and corrected to zero baseline using routines embedded in Abi 4000 Series Explorer Software v3.6. Each PMF spectrum was internally calibrated with the mass signals of trypsin autolysis ions to reach a typical mass measurement accuracy of <25 p.p.m. Known trypsin and keratin mass signals, as well as potential sodium and potassium adducts (+21 Da and +39 Da) were removed from the peak list.

To submit the combined PMF and MS/MS data to MASCOT software v.2.1 (Matrix Science, London, UK), GPS Explorer v4.9 was used, searching in the non-redundant NCBI protein database (Viridiplantae) with peptide mass tolerance of 75 p.p.m. for MALDI–TOF/TOF analysis.

The remaining 80% of the samples were analysed by LC coupled to electrospray ion-trap mass spectrometry MS/MS using Ultimate 3000 nano LC (Dionex, Amsterdam, The Netherlands) and a 75-mm I.D., 100 mm reverse-phase column, at 300 nl min⁻¹ flow, coupled to a Bruker HCT Ultra ion-trap mass spectrometer (Bruker Daltonics, Bremen, Germany) working in dynamic exclusion mode. For protein identification, LC coupled to electrospray ion-trap mass spectrometry MS/MS spectra were transferred to BioTools 2.0 interface (Bruker Daltonics), to search in the NCBIInr database using a licensed version of Mascot v.2.2.04 search engine (www.matrixscience.com; Matrix Science). Search parameters were set as follows: in reduced samples, carbamidomethyl cysteine was set as fixed modification by the treatment with iodoacetamide, oxidized methionines as variable modification, peptide mass tolerance of 0.5 Da for the parental mass and fragment masses, and one missed cleavage site. In the case of non-reduced samples, biotin-HPDP cysteine modification was set as variable modification.

Yeast two-hybrid assay. ABI5 and ABI5C153S were cloned in the pDEST22 and pDEST32 vectors using the GATEWAY technology. Prey and bait clones were grown for 3 days on DOB-W and DOB-L (MP Biomedicals) plates from their corresponding frozen stocks. YPAD medium was inoculated in parallel with bait and prey cells, and incubated overnight at 28°C with shaking (200 r.p.m.). After overnight incubation, the bait culture was added to prey and mating was allowed 48 h by incubating at 28°C without shaking. Settled cells were resuspended and used to inoculate plates containing diploid selection media (DOB-L-W). After 1 day of growth at 28°C and vigorous shaking, diploid cells were resuspended and spotted onto diploid selection and screening (DOB-L-W–Histidine \pm 3-Amino-1,2,4-triazole; 3-AT, Sigma) plates. Positive colonies were visible after 2–5 days of growth at 28°C .

Electrophoretic mobility shift assay. For the electrophoretic mobility shift assay, 10 ng of a double-stranded biotinylated probe 5'-GATCCTCTCGCGTACAA-TAAAGTCAGACACGTGGCATGTCACCAACGTAGCGTATGCGTA-3'(ABRE-binding site motif underlined)³⁶ was incubated with 1.5 μ g wild-type ABI5 or mutant ABI5C153S recombinant protein in the presence and absence of GSNO (1 mM) and DTT (1 mM) as described previously³⁷. Basically, DNA-binding reactions were performed in a buffer containing 10 mM Tris, pH 8, 1 mM EDTA, 100 mM NaCl, 2 mM DTT and 10% glycerol. Protein extracts were mixed with labelled DNA, 0.5 μ g poly(dI-dC) and BSA (250 μ g μ l⁻¹) and incubated for 30 min on ice. Electrophoretic mobility shift assay to separate free and bound DNA was in 6% polyacrylamide gel (40:1 bisacrylamide cast in $0.5 \times$ TBE; TBE is 89 mM Tris, 89 mM boric acid and 2 mM EDTA).

Co-immunoprecipitation and pull-down assays. For haemagglutinin (HA) and FLAG pull-down assays, the proteins were extracted with lysis buffer (100 mM Tris–HCl, pH 7.5, 150 mM NaCl, 0.1% Tween-20) supplemented with 1 mM phenylmethanesulfonyl fluoride and protease inhibitors (Roche). Extracts were cleared by centrifugation and protein concentration was determined by Bradford assay. One milligram of soluble proteins was treated with GSNO (1 mM) in darkness at room temperature during 1 h. After treatment, extracts were immunoprecipitated using anti-HA Affinity Matrix (Roche) and anti-FLAG M2 Matrix (Sigma) for ABI5/KEG and ABI5/CUL4 interactions, respectively. Extracts and beads were incubated during 2 h at 4°C and beads were washed two times in lysis buffer. Next, the beads were incubated at 4°C during 2 h with 1 mg of ABI5 and ABI5C153S soluble proteins previously treated with GSNO (1 mM) in darkness at room temperature during 1 h. After incubation, beads were washed three times in lysis buffer and proteins were eluted from beads in SDS sample buffer. The proteins were visualized using anti-MYC antibodies (Abcam ab62928, 1:10,000), anti-HA antibodies (Roche 12013819001, 1:2,000) and anti-FLAG antibodies (Sigma F1804, 1:1,000).

Generation of transgenic *Arabidopsis* plants. ABI5 and ABI5C153S were cloned in the pEarleyGate 203 vector³⁸ using the GATEWAY technology and the following primers (ABI5-F 5'-ATGGTAACTAGAGAAACGAAAGTTGACG-3'; ABI5-R 5'-TTAGAGTGGACAACCTCGGG-3'). Similarly, ABI5_{pro}-ABI5 was cloned in the binary pGWB3 vector³⁹ fused to *GUS*. The constructs generated (Supplementary Fig. 11a) were used to transform the C58C1 (pGV2260) *Agrobacterium* strain⁴⁰. For plant transformation, *Arabidopsis* plants (Col-0, *abi5-1* or *abi5-7*) were transformed by the floral dip method⁴¹ as described previously⁴². Seeds were harvested and plated on selection medium to identify T1 transgenic plants. Approximately 100 of the T2 seeds were plated on selection medium MS agar plates and transgenic lines with a 3:1 (resistant/sensitive) segregation ratio were selected. T3 progenies homozygous for selection medium resistance were used for further studies.

References

- Nambara, E. *et al.* Abscisic acid and the control of seed dormancy and germination. *Seed Sci. Res.* **20**, 55–67 (2010).
- Lopez-Molina, L., Mongrand, S. & Chua, N. H. A post-germination developmental arrest checkpoint is mediated by abscisic acid and requires the ABI5 transcription factor in *Arabidopsis*. *Proc. Natl Acad. Sci. USA* **98**, 4782–4787 (2001).

3. Finkelstein, R. R. & Lynch, T. J. The *Arabidopsis* abscisic acid response gene *ABI5* encodes a basic leucine zipper transcription factor. *Plant Cell* **12**, 599–609 (2000).
4. Benschmih, S. *et al.* The homologous *ABI5* and *EEL* transcription factors function antagonistically to fine-tune gene expression during late embryogenesis. *Plant Cell* **14**, 1391–1403 (2002).
5. Lopez-Molina, L., Mongrand, S., McLachlin, D., Chait, B. & Chua, N. H. *ABI5* acts downstream of *ABI3* to execute an ABA-dependent growth arrest during germination. *Plant J.* **32**, 1–12 (2002).
6. Wang, P. *et al.* Nitric oxide negatively regulates abscisic acid signaling in guard cells by S-nitrosylation of *OST1*. *Proc. Natl Acad. Sci. USA* **112**, 613–618 (2014).
7. Gibbs, D. J. *et al.* Nitric oxide sensing in plants is mediated by proteolytic control of group VII ERF transcription factors. *Mol. Cell* **53**, 369–379 (2014).
8. Bethke, P. C., Badger, M. R. & Jones, R. L. Apoplastic synthesis of nitric oxide by plant tissues. *Plant Cell* **16**, 332–341 (2004).
9. Bethke, P. C., Gubler, F., Jacobsen, J. V. & Jones, R. L. Dormancy of *Arabidopsis* seeds and barley can be broken by nitric oxide. *Planta* **219**, 847–855 (2004).
10. Beligni, M. V. & Lamattina, L. Nitric oxide stimulates seed germination and de-etiolation, and inhibits hypocotyl elongation, three light-inducible responses in plants. *Planta* **210**, 215–221 (2000).
11. Lozano-Juste, J. & Leon, J. Enhanced abscisic acid-mediated responses in *nia1nia2noa1-2* triple mutant impaired in NIA/NR- and AtNOA1-dependent nitric oxide biosynthesis in *Arabidopsis*. *Plant Physiol.* **152**, 891–903 (2010).
12. Stamler, J. S., Lamas, S. & Fang, F. C. Nitrosylation: the prototypic redox-based signaling mechanism. *Cell* **106**, 675–683 (2001).
13. Kwak, Y. D. *et al.* NO signaling and S-nitrosylation regulate PTEN inhibition in neurodegeneration. *Mol. Neurodegener.* **5**, 49 (2010).
14. Liu, Y. G. *et al.* Nitric oxide-induced rapid decrease of abscisic acid concentration is required in breaking seed dormancy in *Arabidopsis*. *New Phytol.* **183**, 1030–1042 (2009).
15. Fernández-Marcos, M., Sanz, L., Lewis, D. R., Muday, G. K. & Lorenzo, O. Nitric oxide causes root apical meristem defects and growth inhibition while reducing PIN-FORMED 1 (PIN1)-dependent acropetal auxin transport. *Proc. Natl Acad. Sci. USA* **108**, 18506–18511 (2011).
16. Hill, R. D. Non-symbiotic haemoglobins—what’s happening beyond nitric oxide scavenging? *AoB Plants* **pl004**, 1–13 (2012).
17. Romero-Puertas, M. C. *et al.* S-nitrosylation of peroxiredoxin II E promotes peroxynitrite-mediated tyrosine nitration. *Plant Cell* **19**, 4120–4130 (2007).
18. Jaffrey, S. R. & Snyder, S. H. The biotin switch method for the detection of S-nitrosylated proteins. *Sci. STKE* **86**, pl1 (2001).
19. Nakamura, S., Lynch, T. J. & Finkelstein, R. R. Physical interactions between ABA response loci of *Arabidopsis*. *Plant J.* **26**, 627–635 (2001).
20. Chen, H. *et al.* *Arabidopsis* CULLIN4 forms an E3 ubiquitin ligase with RBX1 and the CDD complex in mediating light control of development. *Plant Cell* **18**, 1991–2004 (2006).
21. Lee, J. H. *et al.* DWA1 and DWA2, two *Arabidopsis* DWD protein components of CUL4-based E3 ligases, act together as negative regulators in ABA signal transduction. *Plant Cell* **22**, 1716–1732 (2010).
22. Stone, S. L., Williams, L. A., Farmer, L. M., Vierstra, R. D. & Callis, J. KEEP ON GOING, a RING E3 ligase essential for *Arabidopsis* growth and development, is involved in abscisic acid signaling. *Plant Cell* **18**, 3415–3428 (2006).
23. Liu, H. & Stone, S. L. Abscisic acid increases *Arabidopsis* *ABI5* transcription factor levels by promoting KEG E3 ligase self-ubiquitination and proteasomal degradation. *Plant Cell* **22**, 2630–2641 (2010).
24. Liu, H. & Stone, S. L. Cytoplasmic degradation of the *Arabidopsis* transcription factor ABCISIC ACID INSENSITIVE 5 is mediated by the RING-type E3 Ligase KEEP ON GOING. *J. Biol. Chem.* **288**, 20267–20279 (2013).
25. Holman, T. J. *et al.* The N-end rule pathway promotes seed germination and establishment through removal of ABA sensitivity in *Arabidopsis*. *Proc. Natl Acad. Sci. USA* **106**, 4549–4554 (2009).
26. Gibbs, D. J. *et al.* Homeostatic response to hypoxia is regulated by the N-end rule pathway in plants. *Nature* **479**, 415–418 (2011).
27. Perazzolli, M. *et al.* *Arabidopsis* nonsymbiotic hemoglobin AHB1 modulates nitric oxide bioactivity. *Plant Cell* **16**, 2785–2794 (2004).
28. Wawrzynska, A., Christiansen, K. M., Lan, Y., Rodibaugh, N. L. & Innes, R. W. Powdery mildew resistance conferred by loss of the ENHANCED DISEASE RESISTANCE1 protein kinase is suppressed by a missense mutation in *KEEP ON GOING*, a regulator of abscisic acid signaling. *Plant Physiol.* **148**, 1510–1522 (2008).
29. Murashige, T. & Skoog, F. A revised medium for rapid growth and bioassays with tobacco tissue culture. *Physiol. Plant.* **15**, 473–497 (1962).
30. Nambara, E. *et al.* A screen for genes that function in abscisic acid signaling in *Arabidopsis thaliana*. *Genetics* **161**, 1247–1255 (2002).
31. Jefferson, R. A., Kavanagh, T. A. & Bevan, M. W. GUS fusions: β -glucuronidase as a sensitive and versatile gene fusion marker in higher plants. *EMBO J.* **6**, 3901–3907 (1987).
32. Oñate-Sánchez, L. & Vicente-Carbajosa, J. DNA-free RNA isolation protocols for *Arabidopsis thaliana*, including seeds and siliques. *BMC Res. Notes* **1**, 93 (2008).
33. Bradford, M. A rapid and sensitive method for the quantitation of microgram quantities of protein utilizing the principle of protein-dye binding. *Anal. Biochem.* **72**, 248–254 (1976).
34. Ortega-Galisteo, A. P. *et al.* S-Nitrosylated proteins in pea (*Pisum sativum* L.) leaf peroxisomes: changes under abiotic stress. *J. Exp. Bot.* **63**, 2089–2103 (2012).
35. Schevchenko, A., Wilm, M., Vorm, O. & Mann, M. Mass spectrometric sequencing of proteins from silver stained polyacrylamide gels. *Anal. Chem.* **68**, 850–858 (1996).
36. Carles, C. *et al.* Regulation of *Arabidopsis thaliana* *Em* genes: role of *ABI5*. *Plant J.* **30**, 373–383 (2002).
37. Godoy, M. *et al.* Improved protein-binding microarrays for the identification of DNA-binding specificities of transcription factors. *Plant J.* **66**, 700–711 (2011).
38. Earley, K. W. *et al.* Gateway-compatible vectors for plant functional genomics and proteomics. *Plant J.* **45**, 616–629 (2006).
39. Nakagawa, T. *et al.* Development of series of gateway binary vectors, pGWBs, for realizing efficient construction of fusion genes for plant transformation. *J. Biosci. Bioeng.* **104**, 34–41 (2007).
40. Deblaere, R. *et al.* Efficient octopine Ti plasmid-derived vectors for *Agrobacterium*-mediated gene transfer to plants. *Nucleic Acids Res.* **13**, 4777–4788 (1985).
41. Clough, S. J. & Bent, A. F. Floral dip: a simplified method for *Agrobacterium*-mediated transformation of *Arabidopsis thaliana*. *Plant J.* **16**, 735–743 (1998).
42. Saavedra, X. *et al.* The nuclear interactor PYL8/RCAR3 of *Fagus sylvatica* FsPP2C1 is a positive regulator of abscisic acid signaling in seeds and stress. *Plant Physiol.* **152**, 133–150 (2010).

Acknowledgements

We thank Roberto Solano, Salomé Prat, Javier Paz-Ares and Dolores Rodriguez for critical reading of the manuscript and stimulating discussions. We also thank proteomics facility CNB-CSIC for technical proteomic assistance. We are grateful to Luis Lopez-Molina, Xing Wang Deng, Massimo Delledonne and José León for providing seeds and full-length cDNAs. This work was financed by grants BIO2014-57107-R, BIO2011-26940 and CSD2007-00057 (TRANSPLANTA) from the Ministerio de Economía y Competitividad (Spain), EcoSeed Impacts of Environmental Conditions on Seed Quality 'Eco-Seed-311840' ERC.KBBE.2012.1.1-01 and SA239U13 from Junta de Castilla y León (to O.L.). P.A. was supported by a FPU fellowship from the Ministerio de Educación y Ciencia (Spain).

Author contributions

P.A., M.C.R.-P., K.T., I.M., I.S.-V. and E.N. performed research. P.A., M.C.R.-P., K.T., I.M., I.S.-V., E.N. and O.L. analysed data. O.L. designed research, supervised the work and wrote the paper. All authors discussed the results and commented on the manuscript.

Additional information

Supplementary Information accompanies this paper at <http://www.nature.com/naturecommunications>

Competing financial interests: The authors declare no competing financial interests.

Reprints and permission information is available online at <http://npg.nature.com/reprintsandpermissions/>

How to cite this article: Albertos, P. *et al.* S-nitrosylation triggers *ABI5* degradation to promote seed germination and seedling growth. *Nat. Commun.* 6:8669 doi: 10.1038/ncomms9669 (2015).



This work is licensed under a Creative Commons Attribution 4.0 International License. The images or other third party material in this article are included in the article's Creative Commons license, unless indicated otherwise in the credit line; if the material is not included under the Creative Commons license, users will need to obtain permission from the license holder to reproduce the material. To view a copy of this license, visit <http://creativecommons.org/licenses/by/4.0/>